ACS OMEGA

http://pubs.acs.org/journal/acsodf

Article

Discovery of Core-Fucosylated Glycopeptides as Diagnostic Biomarkers for Early HCC in Patients with NASH Cirrhosis Using LC-HCD-PRM-MS/MS

Yifei Tan, Jianhui Zhu, Cristian D. Gutierrez Reyes, Yu Lin, Zhijing Tan, Zuowei Wu, Jie Zhang, Alva Cano, Sara Verschleisser, Yehia Mechref, Amit G. Singal, Neehar D. Parikh, and David M. Lubman*

Cite This: *ACS Omega* 2023, 8, 12467−12480

Read Online

ACCESS | Metrics & More | Article Recommendations | Supporting Information

ABSTRACT: Aberrant changes in site-specific core fucosylation (CF) of serum proteins contribute to cancer development and progression, which enables them as potential diagnostic markers of tumors. An optimized data-dependent acquisition (DDA) workflow involving isobaric tags for relative and absolute quantitation-labeling and enrichment of CF peptides by lens culinaris lectin was applied to identify CF of serum proteins in a test set of patients with nonalcoholic steatohepatitis (NASH)-related cirrhosis (N = 16) and hepatocellular carcinoma (HCC, N = 17), respectively. A total of 624 CF peptides from 343 proteins, with 683 CF sites, were identified in our DDA−mass spectrometry (MS) analysis. Subsequently, 19 candidate CF peptide markers were evaluated by a target parallel reaction-monitoring−MS workflow in a validation set of 58 patients, including NASH-related cirrhosis (N = 29), early-stage HCC (N = 21), and late-stage HCC (N = 8). Significant changes ($p < 0.01$) were observed in four CF peptides between cirrhosis and HCC, where peptide LGSFEGLVn^{160}LTFIHLQHNR from LUM in combination with AFP showed the best diagnostic performance in discriminating HCC from cirrhosis, with an area under curve (AUC) of 0.855 compared to AFP only (AUC = 0.717). This peptide in combination with AFP also significantly improved diagnostic performance in distinguishing early HCC from cirrhosis, with an AUC of 0.839 compared to AFP only (AUC = 0.689). Validation of this novel promising biomarker panel in larger cohorts should be performed.

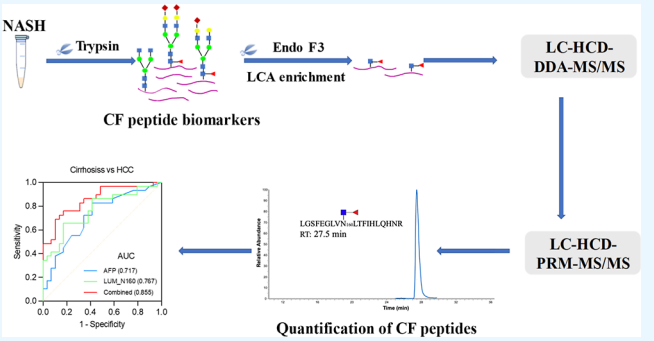

INTRODUCTION

Hepatocellular carcinoma (HCC) is one of the leading causes of cancer-related death worldwide.[1] The early detection of HCC is essential for being able to perform surgical resection or transplantation while those diagnosed at an advanced stage are generally not eligible for curative therapy, with a median survival of 1−2 years.[2] Like most other cancers, early detection of HCC is challenging. HCC surveillance using semiannual ultrasound plus alpha fetoprotein (AFP) is recommended by professional society guidelines given an association with improved early detection and reduced HCC-related mortality; however, this combination misses over one-third of HCC at an early stage.[3]

Due to an unhealthy modern lifestyle, nonalcoholic steatohepatitis (NASH) represents a growing problem and is projected to increase 15−56% globally by 2030, during which advanced liver disease and liver-related mortality will more than double.[4] NASH-related HCC cases experienced an annual increase of 9%[5] in the United States, while in many parts of Asia, HCC is increasingly caused by NASH-related liver disease because of successful hepatitis B virus vaccination programs and urbanization. This shift in cirrhosis and HCC epidemiology is noteworthy given that the imaging quality and sensitivity of ultrasound are significantly impaired in patients with obesity or NASH-related cirrhosis.[6] Therefore, new reliable biomarkers are much needed to complement early detection of NASH-related HCC and improve survival outcomes. Validation of an effective blood-based biomarker could also address issues of surveillance underuse, an issue that is particularly problematic in patients with NASH, thereby further improving surveillance effectiveness for early HCC detection.[7]

In recent years, abnormal changes of glycoproteins and glycopeptides have become of great interest for their diagnostic value in cancers.[8] *N*-Glycosylation is involved in various key pathological processes of carcinogenesis, such as tumor

Received: January 25, 2023
Accepted: March 9, 2023
Published: March 21, 2023

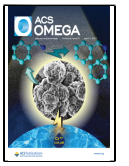

angiogenesis and cell communication.[9] In particular, core fucosylation (CF) has shown promise as a biomarker for various malignancies, including melanoma,[10] lung cancer,[11] pancreatic cancer (PC),[12] and liver cancer.[13] AFP-L3, the CF isoform of AFP, has been approved by the FDA[14] as a biomarker for the diagnosis of HCC. However, AFP-L3 has not contributed significantly to HCC detection, with diagnostic sensitivities of 7.0−41.5% at a cutoff of 5 or 10% in patients with early HCC.[15]

Mass spectrometry (MS)-based large-scale identification of CF peptides has been applied to discover new biomarkers for HCC diagnosis. The difficulty in characterization of serum CF proteins/peptides has involved the complexity of CF and significant suppression by the overwhelming coexistence of nonglycopeptides, particularly considering that complex glycopeptides have significantly reduced ionization efficiency (10−50% of the corresponding nonglycopeptides).[16] A recent report[17] from our research team combined HILIC enrichment and high-pH reversed-phase peptide fractionation to enhance signal intensity of intact glycopeptides in patient sera. Other groups have used one-step lectin enrichment[12,13,18] or MAX solid-phase extraction,[19] followed by Endo F3 digestion. In quantitative proteomics, isobaric tags for relative and absolute quantitation (iTRAQ) labeling has often been used to determine the differences in the expression of CF peptides and was believed to improve identification of targeted peptides by facilitating MS/MS fragmentation.[20] Moreover, targeted MS, such as parallel reaction monitoring (PRM),[21] has been believed to be a promising tool for CF peptide biomarker detection due to its high selectivity and sensitivity.

Yin et al.[13] found that 20 CF peptides were differentially expressed in alcohol (ALC)-related HCC compared to cirrhosis through an iTRAQ labeling-based MS workflow, while 26 CF peptides were significantly changed in HCV-related HCC compared to cirrhosis. CF peptides from isolated serum haptoglobin (Hp)[22] and alpha-1 acid glycoprotein[23] were identified as potential biomarkers for early diagnosis of NASH HCC. However, global-scale identification of CF peptides aberrantly overexpressed in NASH-related HCC serum has not yet been well studied.

In this study, we first performed broad-scale screening for site-specific CF peptides of serum proteins to identify potential biomarkers of detection for early-stage HCC in patients with NASH cirrhosis by introducing a workflow including depletion of high-abundance serum proteins, trypsin digestion, iTRAQ labeling, CF peptide enrichment with LCA, and Endo F3 digestion, followed by C18 desalting and LC-data-dependent acquisition (DDA)-MS/MS. To achieve further quantitative evaluation of the potential CF peptide marker candidates, an optimized LC-PRM-MS/MS workflow has been developed to discover feasible biomarkers for early detection of HCC in patients with NASH.

METHODS

Chemicals and Materials. Trifluoroacetic acid, tris (2-carboxyethyl) phosphine (TCEP), iodoacetamide (IAA), α-methylmannoside, α-methylglucoside, TEAB, Bradford reagents, water [high-performance liquid chromatography (HPLC) grade], formic acid (FA) (HPLC grade), and acetonitrile (HPLC grade) were purchased from Sigma-Aldrich (St. Louis, MO). The Pierce centrifuge column (2 mL), centrifuge filters (0.45 μm), C18 spin column, and low binding tips were purchased from Thermo Fisher Scientific (Fair Lawn, NJ). Low protein-binding tubes were purchased from Eppendorf (Hauppauge, NY). Agarose-bound *Lens culinaris* agglutinin (LCA) was purchased from Vector Laboratories (Burlingame, CA). Amicon ULtra 3 K (0.5 and 4.0 mL) and 10 k (4.0 mL) centrifugal filters were purchased from Millipore (Billerica, MA). The Bradford assay kit was purchased from BioRad (Hercules, CA). iTRAQ 8-plex reagent kits were purchased from AB Sciex (Redwood, CA). Sequencing-grade modified trypsin enzyme was obtained from Promega (Madison, WI). Endoglycosidase F3 (Endo F3) was purchased from BA-Bio (San Mateo, CA). Human 14 multiple affinity removal system spin cartridges for the depletion of high-abundant proteins from human proteomic samples were from Agilent (Santa Clara, CA).

Serum Samples. Human serum samples of cirrhosis and early-stage HCC, all of which were NASH-induced, were provided by UT Southwestern Medical Center, Dallas, Texas, according to institutional review board approval. As previously described, the diagnosis of NASH-induced cirrhosis and HCC was based on radiographic, histologic, and clinical evidence of the corresponding liver diseases, as well as the exclusion of secondary causes[24] (e.g., viral hepatitis and excessive alcohol consumption). The discovery phase included 33 patients with NASH (16 cirrhosis controls and 17 HCC cases), while 58 patients with NASH (29 cirrhosis controls and 29 HCC cases) were used in the validation phase via PRM analysis of serum samples. Patient characteristics of the validation sample set are summarized in Table 1.

Table 1. Demographic and Clinical Information of Validation Sample Set (n = 58)[a]

	Cirrhosis (N = 29)	HCC (N = 29)	P
age	63 (58−67)	68 (61−76)	0.007
male gender (%)	7 (24.1)	10 (34.5)	0.387
creatinine (mg/dL)	0.81 (0.71−1.03)	0.82 (0.69−0.90)	0.348
albumin (g/dL)	3.6 (3.1−4.1)	3.7 (3.2−4.0)	0.868
total bilirubin (mg/dL)	1.35 (0.60−1.83)	0.80 (0.40−1.90)	0.193
ALT	33.0 (30.3−46.3)	42.0 (23.3−49.5)	0.741
AST	47.0 (41.0−66.3)	54.0 (28.5−69.0)	0.724
INR	1.2 (1.1−1.3)	1.1 (1.0−1.2)	0.452
child-Pugh score	6 (5−7)	6 (5−7)	0.935
class A	20 (69.0)	20 (69.0)	1.00
AFP (ng/mL)	3.2 (2.7−5.7)	6.0 (4.0−9.0)	0.267
AFP <20 ng/mL	28 (96.6)	25 (86.2)	0.161
ascites (%)	10 (34.5)	10 (34.5)	1.00
encephalopathy (%)	4 (13.8)	5 (17.2)	0.717
tumor size (cm)	NA	3.9 (2.3−5.7)	
TNM stage (I/II/III)	NA	17/4/8	
presence of cirrhosis	29 (100)	25 (86.2)	0.112

[a]Values are presented as median with the interquartile range. AFP: α-fetoprotein; ALT: alanine aminotransferase; AST: aspartate aminotransferase; and INR: international normalized ratio.

Depletion of High-Abundance Serum Proteins in DDA Workflow. Serum samples were stored at −80 °C and were not thawed until use when 10 μL of each sample was diluted to 200 μL with buffer A. Cell debris and particles were removed first by centrifuging samples through 0.45 μm filters at 9000 g for 1 min. Figure 1A shows the workflow of the screening process which began with the depletion of high-abundance serum proteins.

https://doi.org/10.1021/acsomega.3c00519
ACS Omega 2023, 8, 12467−12480

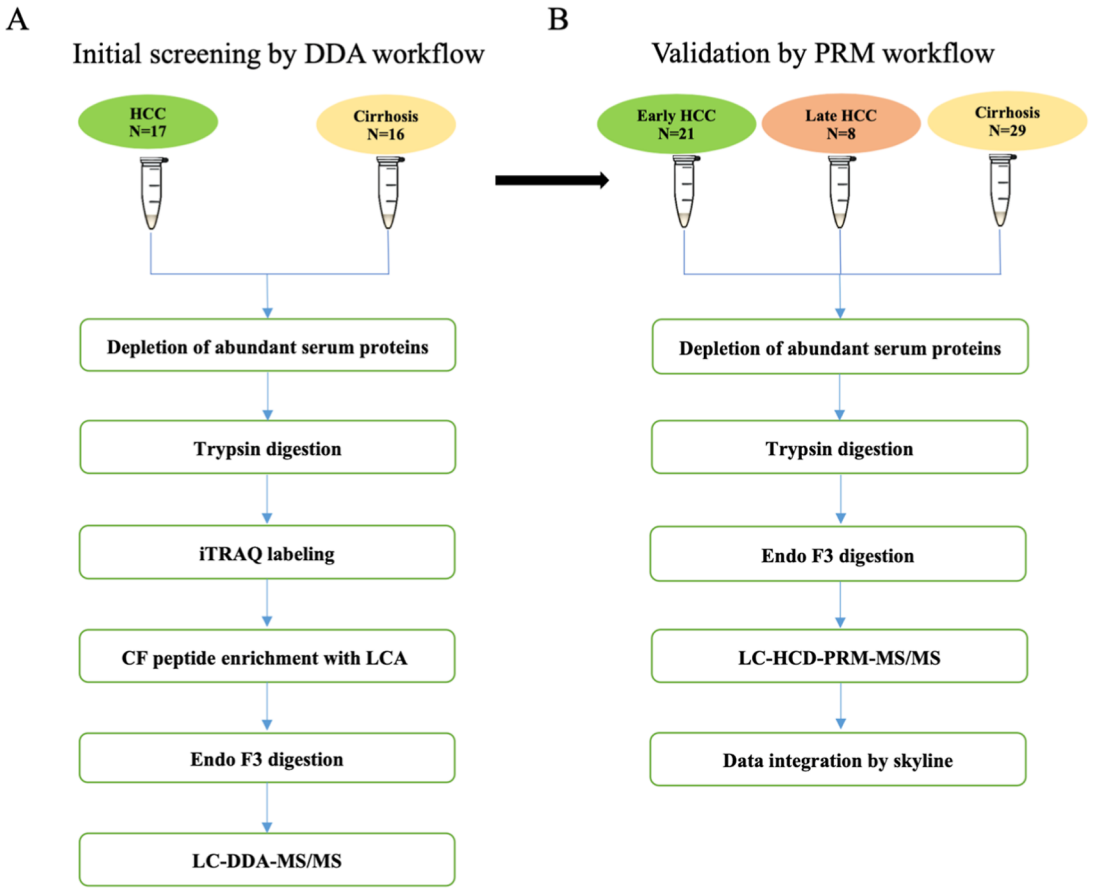

Figure 1. Workflow of quantitative (A) LC-HCD-DDA-MS/MS and (B) LC-HCD-PRM MS/MS analysis of core-fucosylated glycopeptides derived from the serum of patients between NASH-related liver cirrhosis, early-stage HCC, and late-stage HCC.

With a human IgY-7 multiple-affinity removal spin cartridge, the top seven high-abundance serum proteins were depleted following the manufacturer's instructions with some modification. The storage agent in the cartridge was discarded by centrifugation at 100*g* for 1 min before the filter serum sample was loaded. After incubation for 2 min at RT, the sample was centrifuged at 100*g* for 1.5 min where the flow-through fraction was collected. Then, 200 μL of buffer A was loaded to the multiple-affinity spin cartridge and centrifuged at 100*g* for 1.5 min where the fraction was collected, which was repeated twice. Bound fraction (high-abundance proteins) was eluted by 3.0 mL of elution buffer (buffer B) and was discarded, followed by equilibration with 4.0 mL of buffer A.

The depleted serum samples were then transferred to an ultra-4 centrifugal filter (10 kDa MWCO) for desalting. In brief, each sample was diluted to 4.0 mL with HPLC water after being loaded to the filter and centrifuged at 7500*g* for 30 min, followed by buffer exchange with HPLC water for three times. The desalted sample was collected in an Eppendorf tube, and a Bradford assay kit was used to measure protein concentration. Gel electrophoresis with silver staining was applied to confirm the depletion of high-abundance serum protein, with a reference standard protein made by combining bovine serum albumin (1.0 μg/μL) and Hp (0.1 μg/μL).

Trypsin Digestion. Based on the protein concentration, 16 μg of each sample was used for the subsequent trypsin digestion. A pooled sample was derived by mixing 1/15 of each sample and was aliquoted as 16 μg of protein as a reference sample for MS analysis. Urea (8 M) was used to denature the sample to a volume of 100 μL, and then the sample was reduced by adding TCEP to a final concentration of 10 mM and incubated at 37 °C for 30 min. After the sample was cooled to RT, free thiol groups were alkylated by adding 5.0 μL of 0.5 M IAA. The sample was kept in the dark for 30 min at RT before being transferred to an Ultra-0.5 centrifugal filter (3 kDa, MWCO), where buffer exchange was processed. Each sample was buffer exchanged with 500 μL of 50 mM TEAB three times at 14,000 g for 30 min at 4 °C. Subsequently, proteins were digested by 1 μL of sequencing-grade trypsin (0.4 μg/μL) at 37 °C overnight, and the sample was heated at 95 °C for 10 min to deactivate digestion before being dried down in a SpeedVac concentrator (Thermo).

iTRAQ Labeling. The tryptic samples were then labeled with iTRAQ 8-plex isobaric reagents according to manufacturer's instructions. Seven research samples (three or four HCC cases) were randomly assigned to each labeling set with the corresponding iTRAQ tag 114 to 119, while a reference was assigned 121. The samples were afterward incubated at 37 °C for 1 h before adding 0.5 μL of 5% hydroxylamine to quench the reaction at RT for 15 min and dried down by SpeedVac. The eight samples in a set, including a reference, were dissolved with LCA enrichment binding buffer (20 mM Tris HCl, 0.1 M NaCl, pH 7.4, 1 mM CaCl2, 1 mM MnCl2, and 1 mM MgCl2) and pooled. Each pooled sample was afterward buffer exchanged to binding buffer three times on an Ultra-4.0 filter (3 kDa, MWCO) by centrifugation at 7500*g* for 30 min.

https://doi.org/10.1021/acsomega.3c00519
ACS Omega 2023, 8, 12467−12480

LCA Enrichment. Six hundred microliters of agarose-bound LCA slurry were loaded to a 2 mL gravity-flow column (Fisher Scientific, Pittsburgh), where the resin slurry was washed by 1 mL of binding buffer three times. The buffer-exchanged sample was diluted to 500 μL before being transferred to the LCA column and incubated with gentle rotation for 10 min at RT. The flow-through was collected and reloaded to the column for another 10 min incubation. The LCA column[12] was washed with 2 mL of binding buffer four times. Subsequently, the bound CF peptides were eluted twice with 500 μL of elution buffer (binding buffer with 200 mM α-methylglucoside and 200 mM α-methylmannoside) after 10 min incubation. The resin was then eluted by 500 μL of nonionic elution buffer (20 mM Tris with 200 mM α-methylglucoside and 200 mM α-methylmannoside) twice. All eluents were collected and combined, followed by desalting with an Ultra-4.0 centrifugal filter (3 kDa MWCO) at 7500 g for 30 min and dried down by SpeedVac.

Endo F3 Partial Deglycosylation of CF Peptides. Glycans of the enriched CF peptides were cleaved by endoglycosidase F3 (Endo F3). Each sample was dissolved in 30 μL of HPLC water, and 3.5 μL of 10× glycol buffer was added. Two microliters of Endo F3 (8 units/μL) were added to the CF peptides for overnight digestion at 37 °C and dried down with a SpeedVac before desalting with a ZipTip C18 column (Thermo) according to the manufacture's instruction. After eluting, the sample was dried down in a SpeedVac.

Preparation of CF Peptides for LC-HCD-PRM-MS/MS. The validation serum sample set was derived from 29 NASH-HCC and 29 NASH-cirrhosis cases. Samples were depleted and desalted with an Ultra-4.0 centrifugal filter (10 kDa) as described above, and protein concentration was measured. Each sample was dried down by a SpeedVac and then reconstituted in urea solution, followed by reduction with DTT and alkylation with IAA. Around 90 μL of 50 mM ammonium bicarbonate was added to reduce the concentration of urea (<1 M), followed by overnight trypsin digestion at a ratio of 1:50. The sample was desalted four times with an Ultra-0.5 centrifugal filter (3 kDa MWCO) at 14,000g for 30 min, followed by Endo F3 digestion and desalting with a C18 column as described above (Figure 1B).

LC-HCD-DDA-MS/MS Analysis. Each of the 33 samples in the test set for CF peptide screening was dissolved in 20 μL of 0.1% FA before being loaded to a 75 μm × 50 cm column (C18, 2 μm, 100 Å; acclaim PepMap RSLC, Thermo) for LC separation on an Ultimate 3500 UPLC system (ThermoFisher Scientific, San Jose, CA) with a flow rate of 300 nL/min. A binary solvent set consisting of mobile phase A (0.1% FA in H_2O) and B (80% ACN in 0.1% FA) was applied. Peptides were separated through a 90 min linear gradient of mobile B from 5 to 42% in 65 min and 42 to 95% in 5 min, followed by 95% for 5 min to wash and 8% for 10 min to equilibrate the column. The UPLC was coupled with an Orbitrap Fusion Lumos Tribrid Mass Spectrometer which was operated in positive ion mode with the following settings: the Orbitrap resolution for MS1 (m/z 400−1700) scan was 120 k and RF lens was 60%, while a standard AGC and a max injection time of 100 ms were set. Multiple charged precursors detected in the Orbitrap (50 K resolution, m/z 110−2000, 100 ms injection time) were selected for HCD MS/MS (fixed 32% HCD collision energy) according to intensity. Raw data from the MS instrument was acquired using Xcalibur software in data-dependent mode.

LC-HCD-PRM-MS/MS. Settings of LC−MS in the PRM mode were similar with that in the DDA mode. After being resuspended in 2% ACN and 0.1% FA, 5 μL, the processed sample was injected onto a C18 trap column (75 μm × 2 cm, 2 μm, 100 Å; Thermo Scientific, Pittsburgh, PA) for 10 min. The analytical gradient was 60 min long at a flow rate of 350 nL/min, where solvent B (ACN in 0.1% of FA) rose from 3 to 45% in 30 min and from 40 to 80% in 6 min before washing and equilibration. To produce stable and abundant characteristic ions of the core-fucosylated peptides, stepped collision energies (18, 25, and 32%) were set to fragment the glycopeptides. A survey scan was run in DDA−MS/MS to obtain the information of precursor ions and retention times. All the identified precursor ions were included in the PRM-MS method with a retention time window of ±2 min and a mass range of ±2 Da relative to the target mass. All samples were run twice.

Data Interpretation. DDA spectra were analyzed based on a UniProt human protein database which includes 26,152 proteins with Proteome Discoverer 1.4 (Thermo Fisher Scientific, San Jose, CA) software using the Sequest HT search engine. The searching parameters were as follows: (1) dynamic modification: methionine oxidation (+15.995 Da), asparagine glycosylation GlcNac + fucose (+349.137 Da); (2) static modification: lysine and peptide N-terminal iTRAQ labeling (+304.205), cysteine carbamidomethylation (+57.021 Da); (3) mass tolerance: 10 ppm and 0.05 Da for precursor and fragment ion, respectively; (4) one or two missed cleavages were allowed; (5) target FDR: 0.01; (6) quantification method: iTRAQ 8plex; and (7) high-peptide confidence filter.

The specific information for each detected CF peptide structure was targeted in the LC-PRM-MS approach on the Orbitrap Fusion Lumos (Thermo). The selection of the precursor ions for all identified CF peptide structures was based on the signal intensity so that in each case, the most abundant ion was used in the PRM strategy. For all the targets, the fragmentation produced allowed us to confirm the site-specific glycosylation by the observation of abundant Y1 ions, the characteristic HexNAc—fucose residues (m/z 147.1, m/z 184.1, m/z 204.1), and the peptide backbone. Five of the most representative and abundant fragment ions were selected for each CF peptide, and their peak areas were calculated using Xcalibur (Thermo) software. After the area under the curve (AUC) was computed, the differential changes in abundance of the identified CF peptides were investigated in the analyzed samples.

Statistical Analysis. The student t-test and Chi-square test were used in the analysis of continuous and categorical data, respectively, to compare basic information of patients with NASH cirrhosis and NASH HCC. The scatter plots of differentially expressed CF peptides were depicted by GraphPad PRISM 9.0 (La Jolla, CA), while receiver operating characteristic (ROC) curves were generated to evaluate diagnostic efficiency of each target. The AUC with the corresponding specificity and sensitivity was calculated by SPSS 22.0 (IBM, Inc.). A p-value <0.05 was considered to be statistically significant.

RESULTS AND DISCUSSION

Workflow for LC-HCD-DDA-MS/MS and LC-HCD-PRM-MS/MS Analysis. We performed an iTRAQ label-based workflow for the identification of broad-scale CF peptides from

https://doi.org/10.1021/acsomega.3c00519
ACS Omega 2023, 8, 12467−12480

Table 2. CF Peptides and CF Proteins Identified in the Test Set (N = 33)

	no. of CF proteins	no. of CF peptides	CF sites
average of 33 samples	206 ± 17	368 ± 27	387 ± 32
maximum of single run	224	419	433
cirrhosis	206 ± 18	367 ± 25	385 ± 31
HCC	207 ± 17	369 ± 28	388 ± 33
in total	343	624	683

serum samples, including depletion of high-abundance serum proteins, trypsin digestion, iTRAQ labeling, LCA enrichment, and C18 column desalting, followed by LC-HCD-DDA-MS/MS for primary quantitative comparison. Due to the complex nature of serum and the low abundance of CF peptides, immunodepletion of high-abundance proteins combined with enrichment of glycopeptides was adopted to increase the relative abundance of CF peptides. Low-molecular-weight cutoff using an ultracentrifugal filter (3 kDa MWCO) was also applied after trypsin digestion to further reduce nonglycopeptides. The isotopic labeling with iTRAQ enables us to combine eight samples in each set, and the coverage of serum CF peptides was improved because of the significant increase of precursor ions which facilitates detection.

Apart from routine depletion of high-abundance proteins in serum, lectin-based enrichment is another well-established approach to overcome the suppression of nonglycopeptides and indirectly enhances the signals of CF peptides.[25] Notably, our research group optimized the wash and elution step of LCA enrichment, where all resin was completely washed and more CF peptides were recovered by additional elution buffer without NaCl and divalent cations (Mn^{2+}, Ca^{2+}, and Mg^{2+}).[12] Metal ions not only help LCA bind to CF peptides[26] but also negatively affect the release of some CF peptides from the

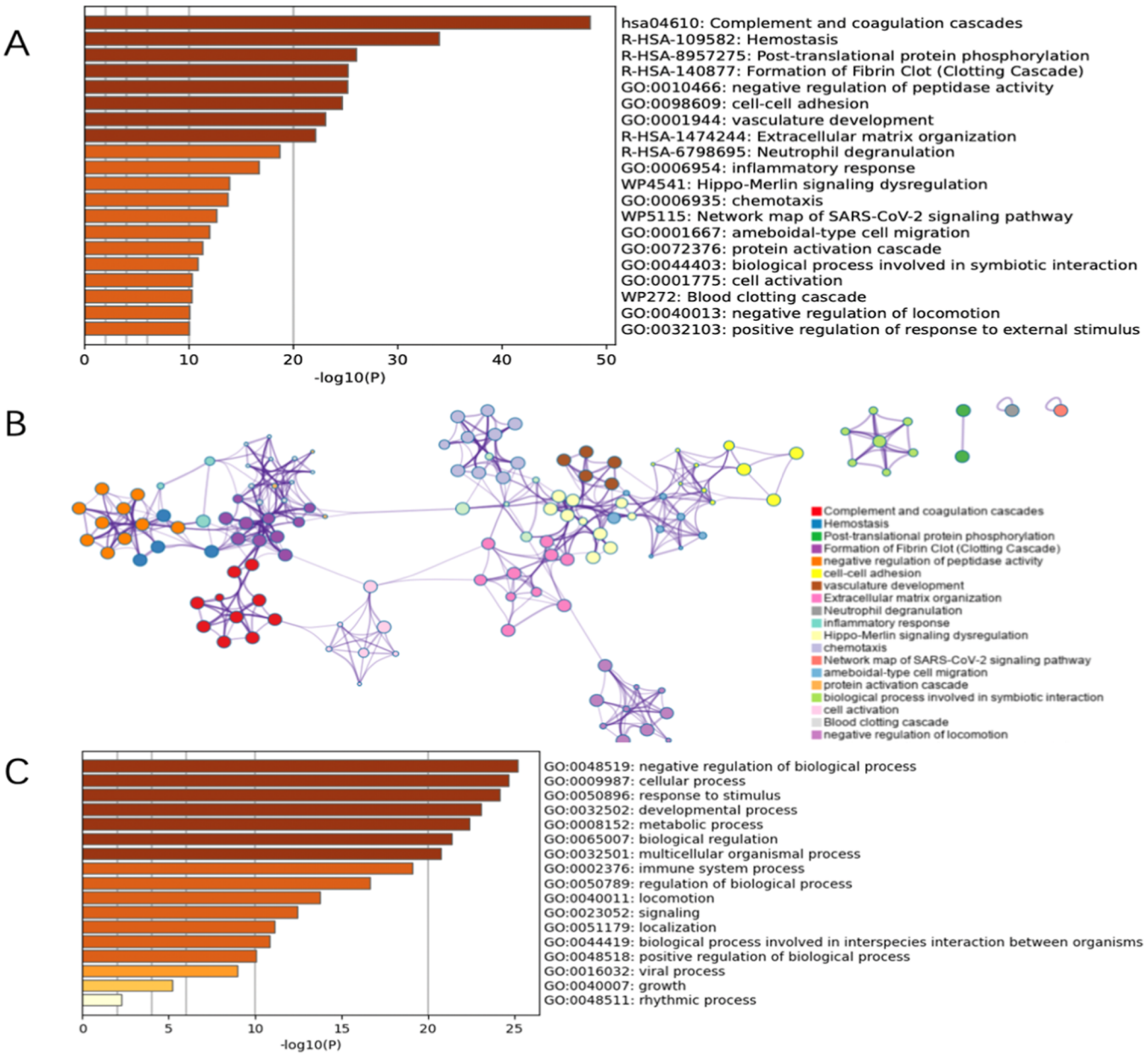

Figure 2. Bar graph (A), network (B) of enriched clusters, and biology process (C) of 343 CF proteins.

https://doi.org/10.1021/acsomega.3c00519
ACS Omega 2023, 8, 12467−12480

Table 3. 28 CF Peptides Found in Different Quantities between Cirrhosis and HCC

protein accessions	CF protein	sequence	HCC/cirrhosis	p
P01871	Ig mu chain C region	THTn^{272}ISESHPn^{279}ATFSAVGEASICEDDWNSGER	1.37	0.008
P26927	hepatocyte growth factor-like protein	GTGNDTVLNVALLn^{625}VISNQECNIK	1.35	0.018
Q92859	neogenin	TLSDVPSAAPQn^{639}LSLEVR	1.27	0.042
P02748	complement component C9	AVn^{415}ITSENLIDDVVSLIR	1.25	0.019
Q9UJV3	probable E3 ubiquitin-protein ligase MID2	QTLEMn^{246}LTNLVK	1.19	0.017
P02745	complement C1q subcomponent subunit A	NPPMGGNVVIFDTVITNQEEPYQn^{146}HSGR	1.17	0.011
P10909	clusterin	EDALn^{86}ETR	0.87	0.037
Q9NZP8	complement C1r subcomponent-like protein	GFLALYQTVAVn^{166}YSQPISEASR	0.85	0.026
P55058	phospholipid transfer protein	GKEGHFYYn^{64}ISEVK	0.84	0.048
Q9H6X2	anthrax toxin receptor 1	DFn^{184}ETQLAR	0.83	0.021
P05362	intercellular adhesion mol 1	An^{145}LTVVLLR	0.83	0.033
Q13740	CD166 antigen	Ln^{91}LSENYTLSISNAR	0.83	0.025
P29622	Kallistatin	SQILEGLGFn^{108}LTELSESDVHR	0.83	0.004
Q9UBG0	C-type mannose receptor 2	WNDSPCn^{497}QSLPSICK	0.83	0.031
P15151	poliovirus receptor	VEDEGn^{120}YTCLFVTFPQGSR	0.82	0.002
Q12884	seprase	DDNLEHYKn^{679}STVMAR	0.82	0.006
Q9P121	neurotrimin	LIFFn^{284}VSEHDYGn*YTCVASNK	0.81	0.033
P43251	biotinidase	DVQIIVFPEDGIHGFn^{119}FTR	0.81	0.005
P01042	kininogen-1	KYNSQn^{48}QSNNQFVLYR	0.80	0.016
P10909	clusterin	LAn^{374}LTQGEDQYYLR	0.80	0.001
		KEDALn^{86}ETR	0.78	0.028
P51884	lumican	LGSFEGLVn^{160}LTFIHLQHNR	0.78	0.037
P33151	cadherin-5	ELDREVYPWYn^{442}LTVEAK	0.78	0.025
Q99784	noelin	VHYAYQTn^{431}ASTYEYIDIPFQNK	0.76	0.050
P01127	platelet-derived growth factor subunit B	LLHGDPGEEDGAELDLn^{63}MTR	0.74	0.013
Q14314	fibroleukin	LHVGNYn^{336}GTAGDALR	0.74	0.022
Q92823	neuronal cell adhesion molecule	ERPPTFLTPEGn^{276}ASNKEELR	0.72	0.021
O00391	sulfhydryl oxidase 1	AFTKn^{130}GSGAVFPVAGADVQTLR	0.67	0.033

lectin, and about one-third of CF peptides were recovered by elution buffer without NaCl and divalent cations.[12]

Our DDA workflow allowed large-scale screening of site-specific CF peptides and provided a list of targeted CF peptides which were primarily identified differentially expressed between HCC and cirrhosis and were further analyzed with PRM workflow in a validation cohort of 58 patients (29 NASH-HCC and 29 NASH-Cirrhosis). Unlike multiple reaction monitoring (MRM)[27,28] that requires preselection of transitions, all transitions of targeted precursor ions are simultaneously monitored in PRM analysis with high resolution and mass accuracy.

Identification of CF Peptides. Raw data from the DDA mode was searched by Proteome Discoverer software, where CF peptides were initially identified based on the presence of precursor ions (HexNAc, +349.137) with high confidence (1% FDR). Diagnostic HexNAc ions were also required for final confirmation of CF sites, including m/z 126.055, m/z 138.055, m/z 186.066, and m/z 204.087. In addition, we excluded redundantly counted CF peptides caused by trypsin miscleavage, which generally occurred when there is a K or R located immediately after another K or R or the glycosylated site.[29] Fourteen duplicated CF sites that resulted from missed cleavage of trypsin were excluded.

The numbers of CF proteins, CF peptides, and CF sites identified in the test set of 33 serum samples with LC-HCD-DDA-MS/MS workflow are summarized in Table 2, and data of site-specific distribution of core-fucosylation regarding proteins, peptides, and CF sites are available in Tables S1 and S2. A total of 624 CF peptides and 683 CF sites from 343 CF proteins were identified in the DDA mode, with an average of 206 (±17) CF proteins, 368 (±27) CF peptides, and 387 (±32) CF sites in each sample. Similar numbers of CF proteins (206 ± 18 vs 207 ± 17, $p > 0.05$), CF peptides (367 ± 25 vs 369 ± 28, $p > 0.05$), and CF sites (385 ± 31 vs 388 ± 33, $p > 0.05$) were observed between the cirrhosis and HCC group. Most CF peptides (92.2%) have only one CF site, while 6.3 and 1.6% of CF peptides have two and three CF sites, respectively.

Ingenuity pathway analysis showed that the clusters of these 343 CF proteins mainly involved complement and coagulation cascades, hemostasis, and post-translational protein phosphorylation (Figure 2A,B). The biological process analysis indicated that these proteins participate in negative biological regulation and cellular processes (Figure 2C).

Comparison of CF Peptides between HCC and Cirrhosis among DDA Data. In the discovery cohort, positive serum AFP (>20 ng/ml) was observed in only one HCC patient (5.9%), revealing the inadequate sensitivity of AFP in NASH-related HCC which was in line with a previous report.[30] Hence, new serum biomarkers are needed to complement current surveillance procedures for NASH-HCC at an early stage. A comparative analysis was performed to explore potential biomarkers for early detection of NASH-related HCC. For each CF peptide/protein, the ratio of the HCC or cirrhosis sample over the standard reference was used to compare target CF peptide/protein between the two groups. In the 33 serum samples analyzed by iTRAQ-based DDA workflow, 6 unique CF peptides from 6 proteins were upregulated in HCC in comparison to cirrhosis, whereas 22 CF peptides from 20 proteins were downregulated in HCC

https://doi.org/10.1021/acsomega.3c00519
ACS Omega 2023, 8, 12467−12480

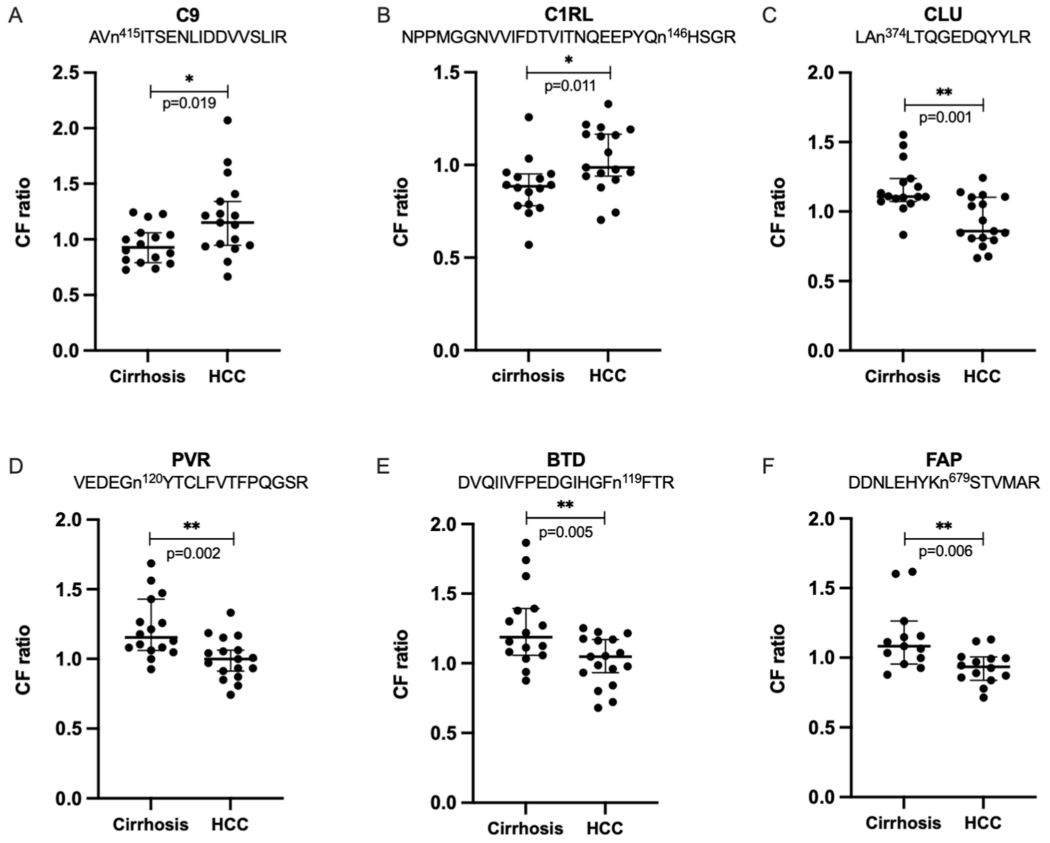

Figure 3. Differentially expressed CF peptides between cirrhosis and HCC in DDA analysis. (A) C9: complement component C9; (B) C1RL: complement C1q subcomponent subunit A; (C) CLU, clusterin; (D) PVR: poliovirus receptor; (E) BTD, biotinidase; and (F) FAP: seprase; *, $P < 0.05$; **, $P < 0.01$.

Table 4. PRM Information for Each of the Targeted CF Peptides

protein	CF peptide	charge	RT (min)	precursor ion (m/z)
complement C1q subcomponent subunit A	NPPMGGNVVIFDTVITNQEEPYQn^{146}HSGR	+3	26.4	1154.8715
kininogen-1	KYNSQn^{48}QSNNQFVLYR	+3	20.1	784.7121
inter-alpha-trypsin inhibitor heavy chain H4	LPTQn^{517}ITFQTESSVAEQEAEFQSPK	+3	28.3	1053.4987
clusterin	EDALn^{86}ETR	+2	15.9	648.7965
clusterin	LAn^{374}LTQGEDQYYLR	+2	23.8	1016.9863
phospholipid transfer protein	GKEGHFYYn^{64}ISEVK	+3	20.6	673.9880
lumican	LGSFEGLVn^{160}LTFIHLQHNR	+4	27.5	636.8313
lumican	AFENVTDLQWLILDHn^{100}LLENSK	+3	29.8	987.8276
lumican	LSHNELADSGIPGn^{249}SFNVSSLVELDLSYNK	+3	29.7	1190.2401
lumican	LHINHNn^{127}*LTESVGPLPK	+4	21.2	558.7911
complement component C9	AVn^{415}ITSENLIDDVVSLIR	+3	32.9	774.0796
anthrax toxin receptor 1	DFn^{184}ETQLAR	+2	21.2	721.8361
intercellular adhesion molecule 1	An^{145}LTVVLLR	+2	17.5	674.3930
complement C1r subcomponent-like protein	GFLALYQTVAVn^{166}YSQPISEASR	+3	26.3	921.8026
kallistatin	DFYVDEn^{238}TTVR	+2	20.1	854.3829
sulfhydryl oxidase 1	AFTKn^{130}GSGAVFPVAGADVQTLR	+3	37.0	852.4445
neuronal cell adhesion molecule	ERPPTFLTPEGn^{276}ASNKEELR	+4	28.7	659.3317
fibronectin	HEEGHMLn^{542}CTCFGQGR	+4	19.1	571.2393
seprase	DDNLEHYKn^{679}STVMAR	+4	19.6	536.2507

samples (Table 3). Figure 3 shows two upregulated and four downregulated CF peptides in HCC compared to cirrhosis.

Even though the labeling-based DDA workflow is powerful in unbiased identification of CF peptides, it is less reliable in acquiring consistent data of interesting CF peptides across samples due to complex preparation steps and its stochastic nature of signal screening. However, DDA provided necessary information of CF peptides for subsequent targeted MS analysis, including amino acid sequence with the corresponding retention time and distribution of reporter ions in the MS^2 spectrum.

Validation of Potential CF Peptide Biomarkers for Distinguishing HCC from Cirrhosis by LC-HCD-PRM-MS/MS. A pooled sample was analyzed in DDA mode and used to

https://doi.org/10.1021/acsomega.3c00519
ACS Omega 2023, 8, 12467−12480

Table 5. Diagnostic Performance of CF Peptides in Identifying HCC from Cirrhosis[a]

protein	CF peptides	HCC/cirrhosis	*p*	AUC	Sensitivity	specificity
AFP				0.717	0.724	0.655
ITIH4	LPTQn[517]ITFQTESSVAEQEAEFQSPK	1.31	0.0057	**0.723**	0.793	0.655
CF-pep + AFP				0.781	0.793	0.655
C9	AVn[415]ITSENLIDDVVSLIR	1.40	0.0014	**0.749**	0.828	0.655
CF-pep + AFP				0.768	0.793	0.690
C1RL	GFLALYQTVAVn[166]YSQPISEASR	1.40	0.0010	**0.727**	0.724	0.690
CF-pep + AFP				0.787	0.759	0.655
LUM	LGSFEGLVn[160]LTFIHLQHNR	0.689	0.0016	**0.767**	0.655	0.828
CF-pep + AFP				0.855	0.724	0.862
NRCAM	ERPPTFLTPEGn[276]ASNKEELR	1.34	0.0211	0.659	0.724	0.621
CF-pep + AFP				0.718	0.621	0.655
FN1	HEEGHMLn[542]CTCFGQGR	2.39	0.0180	0.618	0.517	0.724
CF-pep + AFP				0.755	0.828	0.621
CLU	EDALn[86]ETR	2.38	0.0262	0.636	0.552	0.724
CF-pep + AFP				0.757	0.759	0.655

[a]ITIH4: inter-alpha-trypsin inhibitor heavy chain H4; C9: complement component C9; C1RL: complement C1r subcomponent-like protein; NRCAM: neuronal cell adhesion molecule; FN1: fibronectin; CLU: clusterin; and LUM: lumican.

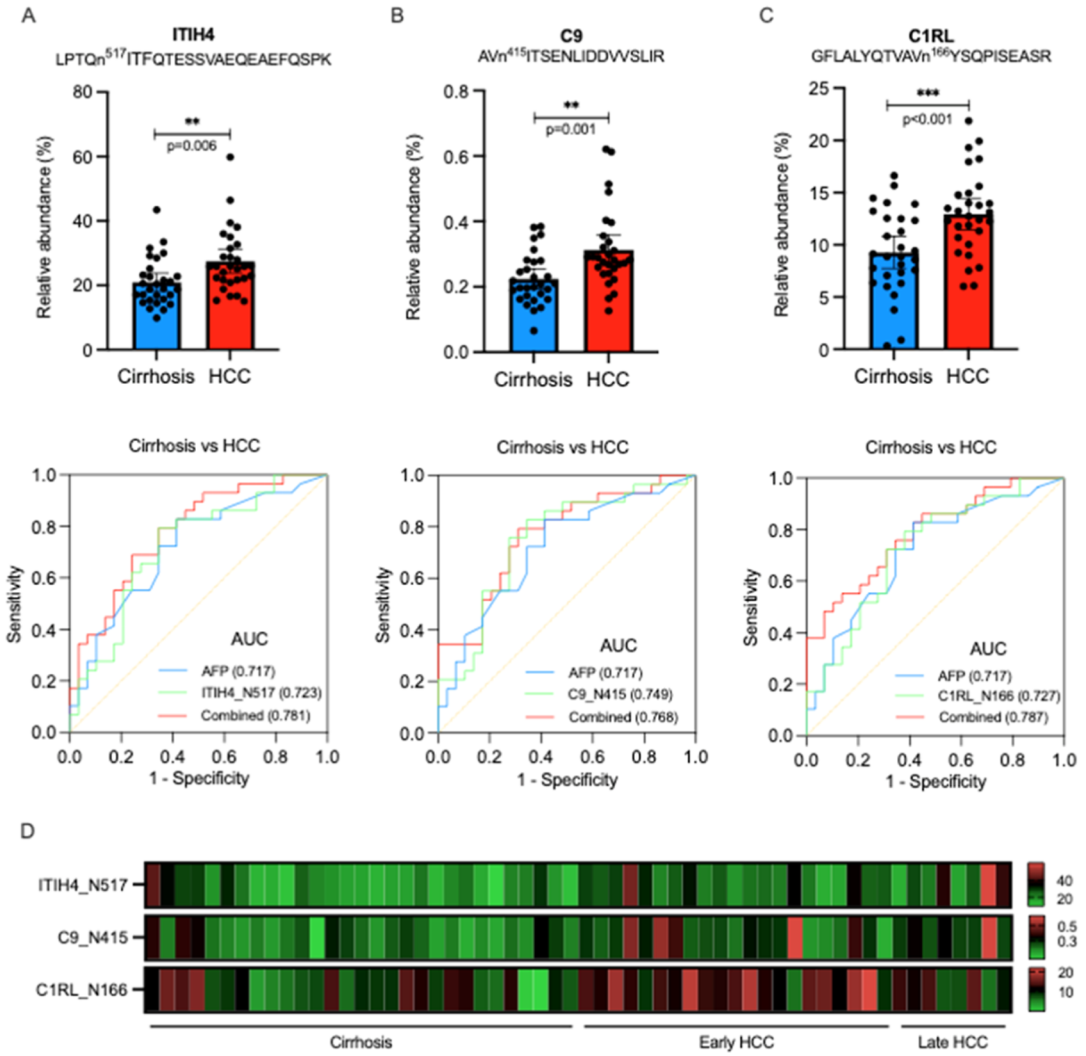

Figure 4. Three upregulated CF peptides in HCC compared with cirrhosis patients and their diagnostic performances in distinguishing HCC from cirrhosis. (A) LPTQn[517]ITFQTESSVAEQEAEFQSPK from ITIH4; (B) AVn[415]ITSENLIDDVVSLIR from C9; and (C) GFLALYQTVAVn[166]YSQPISEASR from C1RL. (D) Heat map of three differentially expressed CF peptides between cirrhosis and HCC. **, $P < 0.01$, ***, $P < 0.001$. ITIH4, inter-alpha-trypsin inhibitor heavy chain H4; C9, complement component C9; and C1RL, complement C1r subcomponent-like protein.

https://doi.org/10.1021/acsomega.3c00519
ACS Omega 2023, 8, 12467−12480

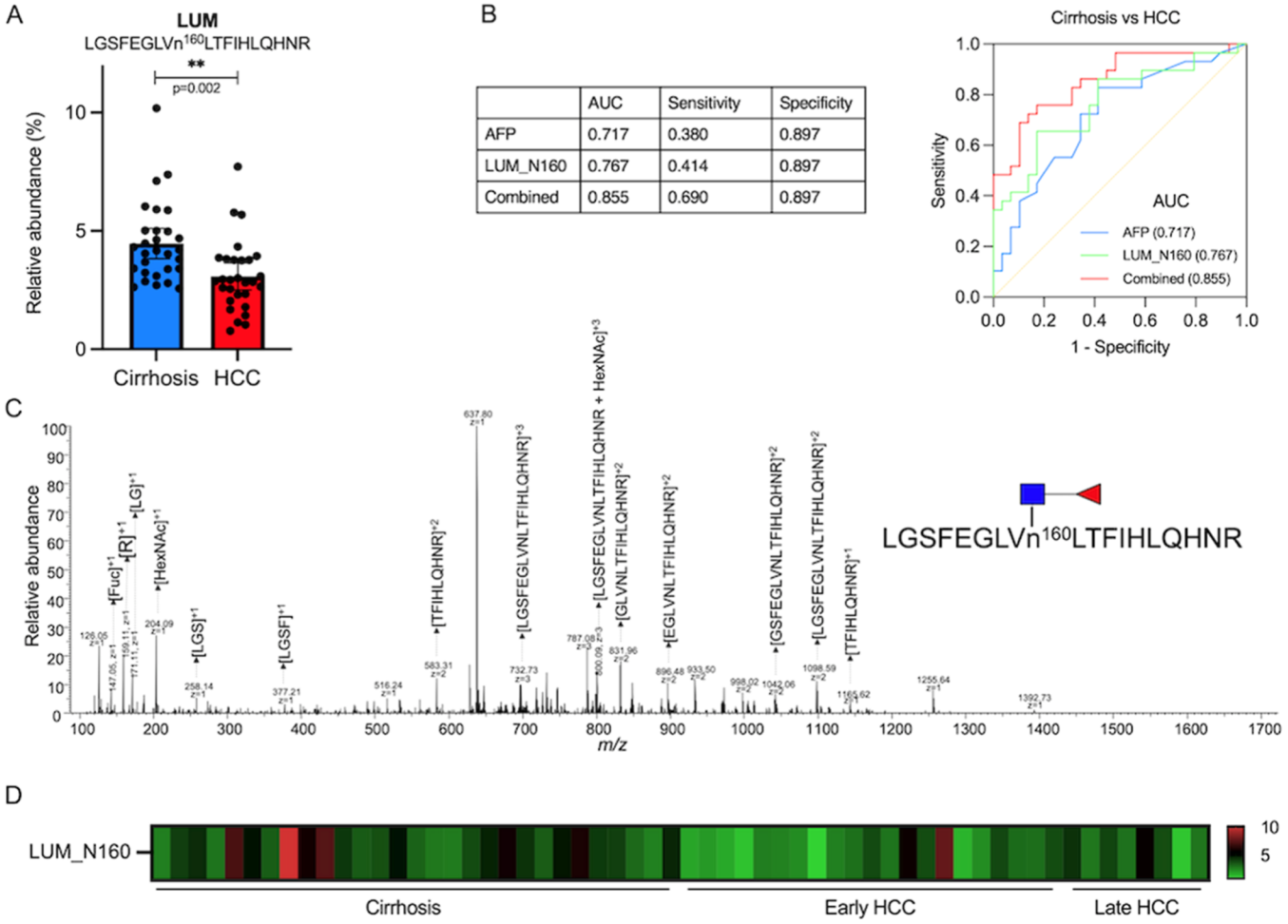

	AUC	Sensitivity	Specificity
AFP	0.717	0.380	0.897
LUM_N160	0.767	0.414	0.897
Combined	0.855	0.690	0.897

Figure 5. (A) Relative abundance of CF peptide LGSFEGLVn[160]LTFIHLQHNR in cirrhosis and HCC patients, respectively. (B) ROC analysis of the CF peptide to differentiate HCC from cirrhosis patients. (C) MS/MS spectrum of LGSFEGLVn[160]LTFIHLQHNR. (D) Heat map of LGSFEGLVn[160]LTFIHLQHNR in cirrhosis and early and late HCC. **, $P < 0.01$.

identify the CF peptides present in the samples based on monoisotopic mass, charge, retention time, and MS^2 spectra (Table 4). A total of 19 CF peptides from 15 proteins, with common extracted ion chromatograms (EICs), were verified by label-free PRM analysis and were analyzed in a validation cohort of 58 samples (29 cirrhosis, 21 early-stage HCC, and 8 late-stage HCC). We compared the relative abundance of each CF peptide between HCC and cirrhosis, which was calculated by normalizing the peak area of certain CF peptides to that of the sum of all targeted CF peptides in the sample.

In the PRM analysis, seven CF peptides were found to be differentially expressed between HCC and cirrhosis, including six peptides that were significantly upregulated in HCC and another one downregulated, with results of ROC analysis listed in Table 5. Comparison in four CF peptides between HCC and cirrhosis resulted in p values less than 0.01 (Figures 4 and 5A), and these CF peptides also showed satisfying performance in distinguishing HCC from cirrhosis. LPTQn[517]ITFQTESSVAEQEAEFQSPK from inter-alpha-trypsin inhibitor heavy chain H4 (ITIH4), yielded an AUC of 0.723 (95% CI: 0.590−0.856) (Figure 4A), while AVn[415]ITSENLIDDVVSLIR from complement component C9 (C9) (Figure 4B) and GFLALYQTVAVn[166]YSQPISEASR from complement C1r subcomponent-like protein (C1RL) (Figure 4C) had AUCs of 0.749 (95% CI: 0.620−0.878) and 0.727 (95% CI: 0.596−0.857), respectively, all outperforming AFP (AUC 0.717, 95%CI: 0.584−0.850). The difference in the only downregulated CF peptide, LGSFEGLVn[160]LTFIHLQHNR from Lumican (LUM), had the best performance in distinguishing HCC from cirrhosis, with an AUC of 0.767 (95% CI: 0.644−0.890) (Figure 5B). Figure 5C shows the corresponding tandem mass spectra of LGSFEGLVn[160]LTFIHLQHNR. Heat maps of the three upregulated CF peptides and the one from LUM are shown in Figures 4D and 5D, respectively.

To distinguish HCC from cirrhosis, AFP had a sensitivity of 72.4% and a specificity of 65.5%. However, when the specificity was set at 89.7%, the sensitivity dropped to only 37.9%, which is not able to effectively detect HCC. The combination analysis with AFP led to an AUC of 0.781 for LPTQn[517]ITFQTESSVAEQEAEFQSPK (Figure 4A), 0.768 for AVn[415]ITSENLIDDVVSLIR (Figure 4B), 0.787 for GFLALYQTVAVn[166]YSQPISEASR (Figure 4C), and 0.855 for LGSFEGLVn[160]LTFIHLQHNR (Figure 5B). The combination with LPTQn[517]ITFQTESSVAEQEAEFQSPK and GFLALYQTVAVn[166]YSQPISEASR improved the sensitivity to 79.31 and 75.86%, respectively, at a specificity of 65.52%. The sensitivity increased to 79.31% when combining AFP and AVn[415]ITSENLIDDVVSLIR, while the specificity was raised to 68.97%. The downregulated CF peptide,

https://doi.org/10.1021/acsomega.3c00519
ACS Omega 2023, 8, 12467−12480

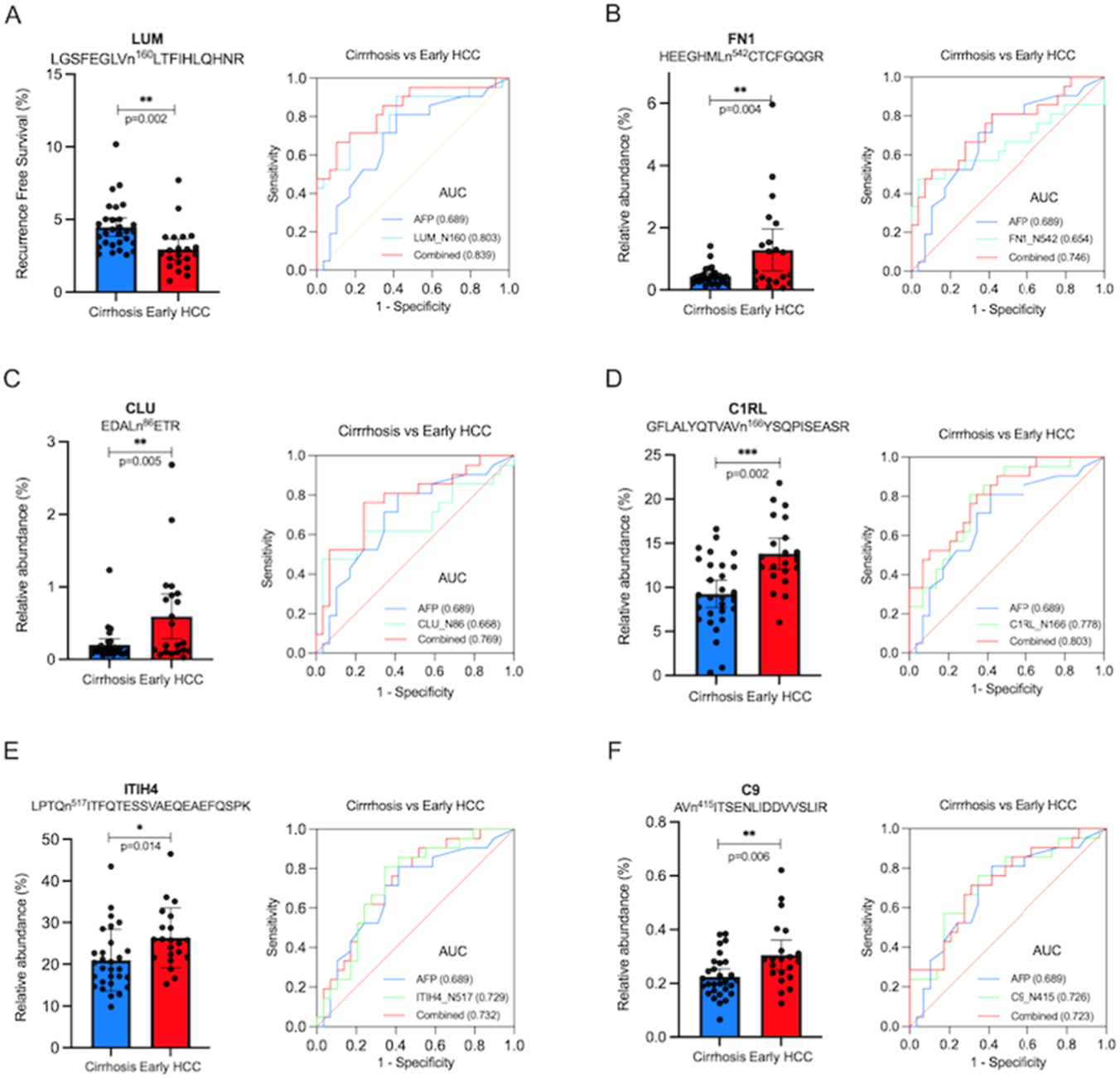

Figure 6. Six differentially expressed CF peptides in HCC compared with cirrhosis patients and their diagnostic performances in distinguishing early HCC from cirrhosis. (A) LGSFEGLVn^{160}LTFIHLQHNR from LUM; (B) HEEGHMLn^{542}CTCFGQGR from FN1; (C) EDALn^{86}ETR from CLU; (D) GFLALYQTVAVn^{166}YSQPISEASR from C1RL; (E) LPTQn^{517}ITFQTESSVAEQEAEFQSPK from ITIH4; and (F) AVn^{415}ITSENLIDDVVSLIR from C9. *, $P < 0.05$, **, $P < 0.01$, ***, $P < 0.001$. LUM, lumican; FN1, fibronectin; CLU, clusterin; C1RL, complement C1r subcomponent-like protein; ITIH4, inter-alpha-trypsin inhibitor heavy chain H4; and C9, complement component C9.

LGSFEGLVn^{160}LTFIHLQHNR, was the best at improving specificity in combination with AFP, which increased specificity to 86.21% at a sensitivity of 72.41%. Even though the AUC of AFP was improved by combining the aforementioned four peptides, only the combination with LGSFEGLVn^{160}LTFIHLQHNR significantly improved the sensitivity to 69.0% at a specificity of 89.7% (Figure 5B), while the other three resulted in even lower sensitivities than AFP alone (data not shown).

In terms of early HCC, AFP had an AUC of 0.689, with a sensitivity of 33.3% at a specificity of 89.7%. LGSFEGLVn^{160}LTFIHLQHNR (Figure 6A) again had the largest AUC of 0.803 in distinguishing early HCC from cirrhosis, with a sensitivity of 52.4% at a specificity of 93.1%, followed by HEEGHMLNCTCFGQGR (Figure 6B) and EDALNETR (Figure 6C), both with a sensitivity of 47.6% at a specificity of 96.6% (Table 6). When combined with AFP, LGSFEGLVn^{160}LTFIHLQHNR resulted in a significantly improved AUC of 0.839 compared to AFP alone, with a sensitivity of 66.7% at a specificity of 89.7%. Three other CF peptides, GFLALYQTVAVn^{166}YSQPISEASR (Figure 6D), HEEGHMLNCTCFGQGR, and EDALNETR also improved the diagnostic performance of AFP to an AUC of 0.803, 0.746, and 0.769 and all with an identical sensitivity of 52.4% at a

https://doi.org/10.1021/acsomega.3c00519
ACS Omega 2023, 8, 12467−12480

Table 6. Diagnostic Performance of CF Peptides in Identifying Early HCC from Cirrhosis[a]

protein	CF peptides	HCC/cirrhosis	p	AUC	sensitivity	specificity
AFP				0.689	0.714	0.655
LUM	LGSFEGLVn^{160}LTFIHLQHNR	0.66	0.00214	0.803	0.714	0.828
CF-pep + AFP				0.839	0.667	0.897
FN1	HEEGHMLn^{542}CTCFGQGR	2.96	0.00378	0.654	0.524	0.828
CF-pep + AFP				0.746	0.524	0.897
CLU	EDALn^{86}ETR	2.99	0.00514	0.668	0.619	0.759
CF-pep + AFP				0.769	0.524	0.897
C1RL	GFLALYQTVAVn^{166}YSQPISEASR	1.49	0.00023	0.778	0.810	0.690
CF-pep + AFP				0.803	0.524	0.897
ITIH4	LPTQn^{517}ITFQTESSVAEQEAEFQSPK	1.25	0.01409	0.729	0.810	0.655
CF-pep + AFP				0.732	0.762	0.621
C9	AVn^{415}ITSENLIDDVVSLIR	1.36	0.00592	0.726	0.762	0.655
CF-pep + AFP				0.723	0.714	0.690

[a]ITIH4: inter-alpha-trypsin inhibitor heavy chain H4; C9: complement component C9; C1RL: complement C1r subcomponent-like protein; NRCAM: neuronal cell adhesion molecule; FN1: fibronectin; CLU: clusterin; and LUM: lumican.

specificity of 89.7%. LPTQn^{517}ITFQTESSVAEQEAEFQSPK (Figure 6E) and AVn^{415}ITSENLIDDVVSLIR (Figure 6F), however, did not improve the diagnostic performance of AFP.

Lumican, a class II small leucine-rich proteoglycans family, is characterized by its 40 kDa core protein comprising leucine-rich repeat motifs which are flanked by cysteine clusters.[31] It is widely found aberrantly regulated in serum and/or tumor tissues of patients with various malignancies and closely correlates with clinicopathological factors and prognosis.[32,33] Lumican serves as an important component of extracellular matrix which serves as a physical barrier to prevent invasion and metastasis of melanoma.[34] Lumican also inhibits angiogenesis[35] and snail-promoted tumor migration by reducing the expression of metalloproteinase 14.[33] In gastric cancer (GC), however, lumican in tumor stroma facilitates GC progression via the activation of integrin β1-FAK signaling pathway and is associated with advanced GC stage and poor survival in human patients.[36] Indeed, the role lumican plays in carcinogenesis and progression is quite tumor-specific, and it shows a dual effect on certain cancers, such as PC. Secreted 70 kDa lumican stimulates proliferation of PC cells by activating ERK, while the phosphorylation of AKT is inhibited. On the other hand, lumican represses tumor invasion via upregulation of integrin α3 expression and enhances adherence to laminin.[32] The correlation between lumican and survival outcomes in PC patients remains controversial,[37] and similar inconsistent results have been observed in patients with lung cancer.[38] Little evidence is available on how lumican affects the biological behavior of liver cancer. A knock down of lumican resulted in reduced migration and invasion ability in liver cancer cells via suppression of the ERK1/JNK pathway;[39] however, its impact in vivo has not been reported yet.

Four CF sites have been reported in lumican, at Asn 88, Asn 127, Asn 160, and Asn 252, respectively. Tan et al.[12] reported that the expression of CF peptide LSHNELADSGIPGNSFn^{252}VSSLVELDLSYNK from lumican is higher in PC or chronic pancreatitis compared with healthy controls. MRM analysis revealed upregulation of CF at N127 of lumican in serum from cirrhotic patients, while no difference was detected in terms of CF peptide AFEN^{88}VTDLQWLILDHNLLENSK of lumican.[28] Herein, we found that the CF peptide of lumican, LGSFEGLVn^{160}LTFIHLQHNR, significantly decreased in serum from HCC patients in comparison with that from cirrhotic patients and effectively improved the diagnostic performance of AFP in discriminating HCC from cirrhosis or early HCC from cirrhosis, with AUCs of 0.855 and 0.839, respectively. The regulation of this last CF peptide was "downregulation", and the same pattern was observed in the DDA results (Table 3), as well in the PRM validation, see Figures 5 and 6. This downregulated CF peptide was a promising supplemental biomarker especially for early HCC as AFP only yielded an AUC of 0.689, with a sensitivity of 33.3% at a specificity of 89.7%.

CONCLUSIONS

A global-scale screening of site-specific CF peptides was achieved in patient sera with NASH-related cirrhosis and HCC, respectively, by the combination of iTRAQ-labeling, CF peptide enrichment by LCA, and LC-HCD-DDA-MS/MS analysis which enabled the improvement of low-abundant CF peptide identification. A total of 624 site-specific CF peptides in 343 proteins were detected, of which 28 were differentially expressed between HCC and cirrhosis. Based on our DDA-MS/MS findings, 19 CF peptides from 15 proteins were further evaluated in a validation set of serum samples, including 29 cirrhosis, 21 early HCC, and 8 late HCC patients, by an optimized LC-HCD-PRM-MS/MS. Four CF peptides were found significantly changed in HCC compared with cirrhosis, where LGSFEGLVn^{160}LTFIHLQHNR from lumican, in combination with AFP, showed the best diagnostic performance in discriminating HCC from cirrhosis, with an AUC of 0.855 and a sensitivity of 69.0% at a specificity of 89.7%. Compared to the inadequate performance of AFP (AUC = 0.689) in the detection of early NASH HCC in this sample set, the CF peptide LGSFEGLVn^{160}LTFIHLQHNR remains as a promising biomarker candidate (AUC = 0.839) which warrants further validation.

ASSOCIATED CONTENT

Supporting Information

The Supporting Information is available free of charge at https://pubs.acs.org/doi/10.1021/acsomega.3c00519.

Core-fucosylated proteins identified in sera from NASH patients (16 cirrhosis and 17 HCC); core-fucosylated peptides and the corresponding glycol distribution identified in sera from NASH patients (16 cirrhosis and 17 HCC); and common EICs of 19 selected CF

https://doi.org/10.1021/acsomega.3c00519
ACS Omega 2023, 8, 12467−12480

peptides of an HCC patient and their elution times (XLSX)

AUTHOR INFORMATION

Corresponding Author

David M. Lubman − *Department of Surgery, University of Michigan Medical Center, Ann Arbor, Michigan 48109, United States;* orcid.org/0000-0001-7731-0232; Phone: 734-647-8834; Email: dmlubman@umich.edu; Fax: 734-615-2088

Authors

Yifei Tan − *Department of Liver Surgery, Liver Transplantation Center, West China Hospital of Sichuan University, Chengdu 610017, China; Department of Surgery, University of Michigan Medical Center, Ann Arbor, Michigan 48109, United States*

Jianhui Zhu − *Department of Surgery, University of Michigan Medical Center, Ann Arbor, Michigan 48109, United States;* orcid.org/0000-0002-0051-7777

Cristian D. Gutierrez Reyes − *Department of Chemistry and Biochemistry, Texas Tech University, Lubbock, Texas 79409, United States*

Yu Lin − *Department of Surgery, University of Michigan Medical Center, Ann Arbor, Michigan 48109, United States*

Zhijing Tan − *Department of Surgery, University of Michigan Medical Center, Ann Arbor, Michigan 48109, United States;* orcid.org/0000-0003-3618-5388

Zuowei Wu − *Department of Surgery, University of Michigan Medical Center, Ann Arbor, Michigan 48109, United States*

Jie Zhang − *Department of Surgery, University of Michigan Medical Center, Ann Arbor, Michigan 48109, United States*

Alva Cano − *Department of Internal Medicine, University of Texas Southwestern Medical Center, Dallas, Texas 75390, United States*

Sara Verschleisser − *Department of Internal Medicine, University of Texas Southwestern Medical Center, Dallas, Texas 75390, United States*

Yehia Mechref − *Department of Chemistry and Biochemistry, Texas Tech University, Lubbock, Texas 79409, United States;* orcid.org/0000-0002-6661-6073

Amit G. Singal − *Department of Internal Medicine, University of Texas Southwestern Medical Center, Dallas, Texas 75390, United States*

Neehar D. Parikh − *Department of Internal Medicine, University of Michigan Medical Center, Ann Arbor, Michigan 48109, United States*

Complete contact information is available at: https://pubs.acs.org/10.1021/acsomega.3c00519

Notes

The authors declare the following competing financial interest(s): Amit G. Singal served on advisory board or consultant for Genentech, AstraZeneca, Eisai, Exelixis, Bayer, Glycotest, Exact Sciences, FujiFilm Medical Sciences, Roche, Freenome, and GRAIL; Neehar D. Parikh served for Exelixis, Bayer, Exact Sciences, Freenome, Fujifilm Medical.

ACKNOWLEDGMENTS

We acknowledge the support of this work from the National Cancer Institute under grants 1R01 CA160254 (D.M.L.), U01 CA225753 (D.M.L.), and R50 CA221808 (J.Z.). This work is also supported by the National Institutes of Health, NIH (1R01GM112490-08 and 1R01GM130091-04). This work is also partially supported by the Robert A. Welch Foundation under grant no. D-0005 and the CH Foundation. The Orbitrap instrument was purchased under an NIH shared instrumentation grant S10OD021619. Dr. Singal acknowledges the support from the National Cancer Institute under grant U01 CA271887 and U01 CA230694 (AGS). Dr. Parikh acknowledges the support from the National Cancer Institute under grant U01CA271887 and U01CA230669. DML acknowledges support under the Maud T. Lane Professorship.

ABBREVIATIONS

CF, core fucosylation; LCA, lens culinaris lectin; NASH, nonalcoholic steatohepatitis; HCC, hepatocellular carcinoma; AFP, α-fetoprotein; MS, mass spectrometry; PRM, parallel reaction monitoring; iTRAQ, isobaric tags for relative and absolute quantitation; Endo F3, endoglycosidase F3; ROC, receiver operating characteristic; AUC, area under curve

REFERENCES

(1) Ferlay, J.; Soerjomataram, I.; Dikshit, R.; Eser, S.; Mathers, C.; Rebelo, M.; Parkin, D. M.; Forman, D.; Bray, F. Cancer incidence and mortality worldwide: sources, methods and major patterns in GLOBOCAN 2012. *International journal of cancer* **2015**, *136*, E359−E386.

(2) Finn, R. S.; Qin, S.; Ikeda, M.; Galle, P. R.; Ducreux, M.; Kim, T. Y.; Kudo, M.; Breder, V.; Merle, P.; Kaseb, A. O.; et al. Atezolizumab plus Bevacizumab in Unresectable Hepatocellular Carcinoma. *N Engl J Med* **2020**, *382*, 1894−1905.

(3) (a) Kim, S. Y.; An, J.; Lim, Y. S.; Han, S.; Lee, J. Y.; Byun, J. H.; Won, H. J.; Lee, S. J.; Lee, H. C.; Lee, Y. S. MRI With Liver-Specific Contrast for Surveillance of Patients With Cirrhosis at High Risk of Hepatocellular Carcinoma. *JAMA Oncol* **2017**, *3*, 456−463. (b) Singal, A. G.; Conjeevaram, H. S.; Volk, M. L.; Fu, S.; Fontana, R. J.; Askari, F.; Su, G. L.; Lok, A. S.; Marrero, J. A. Effectiveness of hepatocellular carcinoma surveillance in patients with cirrhosis. *Cancer Epidemiol Biomarkers Prev* **2012**, *21*, 793−799.

(4) Estes, C.; Anstee, Q. M.; Arias-Loste, M. T.; Bantel, H.; Bellentani, S.; Caballeria, J.; Colombo, M.; Craxi, A.; Crespo, J.; Day, C. P.; et al. Modeling NAFLD disease burden in China, France, Germany, Italy, Japan, Spain, United Kingdom, and United States for the period 2016-2030. *J Hepatol* **2018**, *69*, 896−904.

(5) Younossi, Z. M.; Otgonsuren, M.; Henry, L.; Venkatesan, C.; Mishra, A.; Erario, M.; Hunt, S. Association of nonalcoholic fatty liver disease (NAFLD) with hepatocellular carcinoma (HCC) in the United States from 2004 to 2009. *Hepatology (Baltimore, Md* **2015**, *62*, 1723−1730.

(6) Schoenberger, H.; Chong, N.; Fetzer, D. T.; Rich, N. E.; Yokoo, T.; Khatri, G.; Olivares, J.; Parikh, N. D.; Yopp, A. C.; Marrero, J. A.; et al. Dynamic Changes in Ultrasound Quality for Hepatocellular Carcinoma Screening in Patients With Cirrhosis. *Clin Gastroenterol Hepatol* **2022**, *20*, 1561−1569.

(7) (a) Marquardt, P.; Liu, P. H.; Immergluck, J.; Olivares, J.; Arroyo, A.; Rich, N. E.; Parikh, N. D.; Yopp, A. C.; Singal, A. G. Hepatocellular Carcinoma Screening Process Failures in Patients with Cirrhosis. *Hepatol Commun* **2021**, *5*, 1481−1489. (b) Parikh, N. D.; Tayob, N.; Singal, A. G. Blood-based biomarkers for hepatocellular carcinoma screening: Approaching the end of the ultrasound era? *J Hepatol* **2023**, *78*, 207−216.

(8) Zhu, J.; Warner, E.; Parikh, N. D.; Lubman, D. M. Glycoproteomic markers of hepatocellular carcinoma-mass spectrometry based approaches. *Mass spectrometry reviews* **2019**, *38*, 265−290.

(9) Pinho, S. S.; Reis, C. A. Glycosylation in cancer: mechanisms and clinical implications. *Nat Rev Cancer* **2015**, *15*, 540−555.

(10) Agrawal, P.; Fontanals-Cirera, B.; Sokolova, E.; Jacob, S.; Vaiana, C. A.; Argibay, D.; Davalos, V.; McDermott, M.; Nayak, S.;

Darvishian, F.; et al. A Systems Biology Approach Identifies FUT8 as a Driver of Melanoma Metastasis. *Cancer cell* **2017**, *31*, 804−819.
(11) Li, F.; Zhao, S.; Cui, Y.; Guo, T.; Qiang, J.; Xie, Q.; Yu, W.; Guo, W.; Deng, W.; Gu, C.; et al. alpha1,6-Fucosyltransferase (FUT8) regulates the cancer-promoting capacity of cancer-associated fibroblasts (CAFs) by modifying EGFR core fucosylation (CF) in non-small cell lung cancer (NSCLC). *Am J Cancer Res* **2020**, *10*, 816−837.
(12) Tan, Z.; Yin, H.; Nie, S.; Lin, Z.; Zhu, J.; Ruffin, M. T.; Anderson, M. A.; Simeone, D. M.; Lubman, D. M. Large-scale identification of core-fucosylated glycopeptide sites in pancreatic cancer serum using mass spectrometry. *J Proteome Res* **2015**, *14*, 1968−1978.
(13) Yin, H.; Tan, Z.; Wu, J.; Zhu, J.; Shedden, K. A.; Marrero, J.; Lubman, D. M. Mass-Selected Site-Specific Core-Fucosylation of Serum Proteins in Hepatocellular Carcinoma. *J Proteome Res* **2015**, *14*, 4876−4884.
(14) Füzéry, A. K.; Levin, J.; Chan, M. M.; Chan, D. W. Translation of proteomic biomarkers into FDA approved cancer diagnostics: issues and challenges. *Clin Proteomics* **2013**, *10*, 13.
(15) (a) Marrero, J. A.; Feng, Z.; Wang, Y.; Nguyen, M. H.; Befeler, A. S.; Roberts, L. R.; Reddy, K. R.; Harnois, D.; Llovet, J. M.; Normolle, D.; et al. Alpha-fetoprotein, des-gamma carboxyprothrombin, and lectin-bound alpha-fetoprotein in early hepatocellular carcinoma. *Gastroenterology* **2009**, *137*, 110−118. (b) Toyoda, H.; Kumada, T.; Tada, T.; Kaneoka, Y.; Maeda, A.; Kanke, F.; Satomura, S. Clinical utility of highly sensitive Lens culinaris agglutinin-reactive alpha-fetoprotein in hepatocellular carcinoma patients with alpha-fetoprotein <20 ng/mL. *Cancer Sci* **2011**, *102*, 1025−1031.
(16) (a) Stavenhagen, K.; Hinneburg, H.; Thaysen-Andersen, M.; Hartmann, L.; Silva, D.; Fuchser, J.; Kaspar, S.; Rapp, E.; Seeberger, P. H.; Kolarich, D. Quantitative mapping of glycoprotein micro-heterogeneity and macro-heterogeneity: an evaluation of mass spectrometry signal strengths using synthetic peptides and glycopeptides. *J Mass Spectrom* **2013**, *48*, 627−639. (b) Cao, L.; Tolić, N.; Qu, Y.; Meng, D.; Zhao, R.; Zhang, Q.; Moore, R. J.; Zink, E. M.; Lipton, M. S.; Paša-Tolić, L.; et al. Characterization of intact N- and O-linked glycopeptides using higher energy collisional dissociation. *Anal Biochem* **2014**, *452*, 96−102.
(17) Lin, Y.; Zhu, J.; Pan, L.; Zhang, J.; Tan, Z.; Olivares, J.; Singal, A. G.; Parikh, N. D.; Lubman, D. M. A Panel of Glycopeptides as Candidate Biomarkers for Early Diagnosis of NASH Hepatocellular Carcinoma Using a Stepped HCD Method and PRM Evaluation. *J Proteome Res* **2021**, *20*, 3278.
(18) Liu, Y.; He, J.; Li, C.; Benitez, R.; Fu, S.; Marrero, J.; Lubman, D. M. Identification and confirmation of biomarkers using an integrated platform for quantitative analysis of glycoproteins and their glycosylations. *J Proteome Res* **2010**, *9*, 798−805.
(19) Cao, L.; Lih, T. M.; Hu, Y.; Schnaubelt, M.; Chen, S. Y.; Zhou, Y.; Guo, C.; Dong, M.; Yang, W.; Eguez, R. V.; et al. Characterization of core fucosylation via sequential enzymatic treatments of intact glycopeptides and mass spectrometry analysis. *Nat Commun* **2022**, *13*, 3910.
(20) (a) Rauniyar, N.; Yates, J. R., 3rd. Isobaric labeling-based relative quantification in shotgun proteomics. *J Proteome Res* **2014**, *13*, 5293−5309. (b) Liu, Y. C.; Tsai, F. J.; Chen, C. J. A rapid, multiplexed kinase activity assay using 8-plex iTRAQ labeling, SPE, and MALDI-TOF/TOF MS. *Analyst* **2020**, *145*, 992−1000.
(21) Yuan, W.; Benicky, J.; Wei, R.; Goldman, R.; Sanda, M. Quantitative Analysis of Sex-Hormone-Binding Globulin Glycosylation in Liver Diseases by Liquid Chromatography-Mass Spectrometry Parallel Reaction Monitoring. *J Proteome Res* **2018**, *17*, 2755−2766.
(22) (a) Zhu, J.; Huang, J.; Zhang, J.; Chen, Z.; Lin, Y.; Grigorean, G.; Li, L.; Liu, S.; Singal, A. G.; Parikh, N. D.; et al. Glycopeptide Biomarkers in Serum Haptoglobin for Hepatocellular Carcinoma Detection in Patients with Nonalcoholic Steatohepatitis. *J Proteome Res* **2020**, *19*, 3452−3466. (b) Reyes, C. D. G.; Huang, Y.; Atashi, M.; Zhang, J.; Zhu, J.; Liu, S.; Parikh, N. D.; Singal, A. G.; Dai, J.; Lubman, D. M.; et al. PRM-MS Quantitative Analysis of Isomeric N-Glycopeptides Derived from Human Serum Haptoglobin of Patients with Cirrhosis and Hepatocellular Carcinoma. *Metabolites* **2021**, *11*, 463.
(23) Liang, J.; Zhu, J.; Wang, M.; Singal, A. G.; Odewole, M.; Kagan, S.; Renteria, V.; Liu, S.; Parikh, N. D.; Lubman, D. M. Evaluation of AGP Fucosylation as a Marker for Hepatocellular Carcinoma of Three Different Etiologies. *Sci Rep* **2019**, *9*, 11580.
(24) Hester, C. A.; Rich, N. E.; Singal, A. G.; Yopp, A. C. Comparative Analysis of Nonalcoholic Steatohepatitis- Versus Viral Hepatitis- and Alcohol-Related Liver Disease-Related Hepatocellular Carcinoma. *J Natl Compr Canc Netw* **2019**, *17*, 322−329.
(25) Huang, Y.; Zhou, S.; Zhu, J.; Lubman, D. M.; Mechref, Y. LC-MS/MS isomeric profiling of permethylated N-glycans derived from serum haptoglobin of hepatocellular carcinoma (HCC) and cirrhotic patients. *Electrophoresis* **2017**, *38*, 2160−2167.
(26) Loris, R.; Hamelryck, T.; Bouckaert, J.; Wyns, L. Legume lectin structure. *Biochim Biophys Acta* **1998**, *1383*, 9−36.
(27) Sanda, M.; Pompach, P.; Brnakova, Z.; Wu, J.; Makambi, K.; Goldman, R. Quantitative liquid chromatography-mass spectrometry-multiple reaction monitoring (LC-MS-MRM) analysis of site-specific glycoforms of haptoglobin in liver disease. *Mol Cell Proteomics* **2013**, *12*, 1294−1305.
(28) Ma, J.; Sanda, M.; Wei, R.; Zhang, L.; Goldman, R. Quantitative analysis of core fucosylation of serum proteins in liver diseases by LC-MS-MRM. *J Proteomics* **2018**, *189*, 67−74.
(29) Lee, J. Y.; Kim, J. Y.; Park, G. W.; Cheon, M. H.; Kwon, K. H.; Ahn, Y. H.; Moon, M. H.; Lee, H. J.; Paik, Y. K.; Yoo, J. S. Targeted mass spectrometric approach for biomarker discovery and validation with nonglycosylated tryptic peptides from N-linked glycoproteins in human plasma. *Mol Cell Proteomics* **2011**, *10*, M111.
(30) Vipani, A.; Lauzon, M.; Luu, M.; Roberts, L. R.; Singal, A. G.; Yang, J. D. Decreasing Trend of Serum α-Fetoprotein Level in Hepatocellular Carcinoma. *Clin Gastroenterol Hepatol* **2022**, *20*, 1177−1179.
(31) Appunni, S.; Anand, V.; Khandelwal, M.; Gupta, N.; Rubens, M.; Sharma, A. Small Leucine Rich Proteoglycans (decorin, biglycan and lumican) in cancer. *Clin Chim Acta* **2019**, *491*, 1−7.
(32) Yamamoto, T.; Matsuda, Y.; Kawahara, K.; Ishiwata, T.; Naito, Z. Secreted 70kDa lumican stimulates growth and inhibits invasion of human pancreatic cancer. *Cancer Lett* **2012**, *320*, 31−39.
(33) Stasiak, M.; Boncela, J.; Perreau, C.; Karamanou, K.; Chatron-Colliet, A.; Proult, I.; Przygodzka, P.; Chakravarti, S.; Maquart, F. X.; Kowalska, M. A.; et al. Lumican Inhibits SNAIL-Induced Melanoma Cell Migration Specifically by Blocking MMP-14 Activity. *PLoS One* **2016**, *11*, No. e0150226.
(34) Brézillon, S.; Radwanska, A.; Zeltz, C.; Malkowski, A.; Ploton, D.; Bobichon, H.; Perreau, C.; Malicka-Blaszkiewicz, M.; Maquart, F. X.; Wegrowski, Y. Lumican core protein inhibits melanoma cell migration via alterations of focal adhesion complexes. *Cancer Lett* **2009**, *283*, 92−100.
(35) Malinowski, M.; Pietraszek, K.; Perreau, C.; Boguslawski, M.; Decot, V.; Stoltz, J. F.; Vallar, L.; Niewiarowska, J.; Cierniewski, C.; Maquart, F. X.; et al. Effect of lumican on the migration of human mesenchymal stem cells and endothelial progenitor cells: involvement of matrix metalloproteinase-14. *PLoS One* **2012**, *7*, No. e50709.
(36) (a) Wang, X.; Zhou, Q.; Yu, Z.; Wu, X.; Chen, X.; Li, J.; Li, C.; Yan, M.; Zhu, Z.; Liu, B.; et al. Cancer-associated fibroblast-derived Lumican promotes gastric cancer progression via the integrin beta1-FAK signaling pathway. *International journal of cancer* **2017**, *141*, 998−1010. (b) Chen, X.; Li, X.; Hu, X.; Jiang, F.; Shen, Y.; Xu, R.; Wu, L.; Wei, P.; Shen, X. LUM Expression and Its Prognostic Significance in Gastric Cancer. *Front Oncol* **2020**, *10*, 605.
(37) (a) Ishiwata, T.; Cho, K.; Kawahara, K.; Yamamoto, T.; Fujiwara, Y.; Uchida, E.; Tajiri, T.; Naito, Z. Role of lumican in cancer cells and adjacent stromal tissues in human pancreatic cancer. *Oncol Rep* **2007**, *18*, 537−543. (b) Li, X.; Truty, M. A.; Kang, Y.; Chopin-Laly, X.; Zhang, R.; Roife, D.; Chatterjee, D.; Lin, E.; Thomas, R. M.; Wang, H.; et al. Extracellular lumican inhibits pancreatic cancer cell growth and is associated with prolonged survival after surgery. *Clin Cancer Res* **2014**, *20*, 6529−6540.

https://doi.org/10.1021/acsomega.3c00519
ACS Omega 2023, 8, 12467−12480

(38) (a) Yang, C. T.; Li, J. M.; Chu, W. K.; Chow, S. E. Downregulation of lumican accelerates lung cancer cell invasion through p120 catenin. *Cell Death Dis* **2018**, *9*, 414. (b) Hsiao, K. C.; Chu, P. Y.; Chang, G. C.; Liu, K. J. Elevated Expression of Lumican in Lung Cancer Cells Promotes Bone Metastasis through an Autocrine Regulatory Mechanism. *Cancers* **2020**, *12*, 233.

(39) Mu, Q. M.; He, W.; Hou, G. M.; Liang, Y.; Wang, G.; Li, C. L.; Liao, B.; Liu, X.; Ye, Z.; Lu, J. L.; et al. Interference of Lumican Regulates the Invasion and Migration of Liver Cancer Cells. *Sichuan Da Xue Xue Bao Yi Xue Ban* **2018**, *49*, 358−363.

https://doi.org/10.1021/acsomega.3c00519
ACS Omega 2023, 8, 12467−12480